Longitudinal high-dimensional analysis identifies biomarkers of response to anti-PD-1 immunotherapy

Run-Ze Li
Macau University of Science and Technology
Xing-Xing Fan
Macau University of Science and Technology
Ze-Bo Jiang
Macau University of Science and Technology
Jumin Huang
Macau University of Science and Technology
Hu-Dan Pan
Macau University of Science and Technology
Lily Yan Wang
Asia Pacific Center of Excellence in Translational Science, Janssen
Yue Fan
Janssen R&D China, 355 Hong Qiao Road, Shanghai 200030, P.R
Hongmei Xu
Asia Pacific Center of Excellence in Translational Science, Janssen
Haopeng Rui
Asia Pacific Center of Excellence in Translational Science, Janssen
Longen Zhou
Asia Pacific Center of Excellence in Translational Science, Janssen
Paul Gavine
Asia Pacific Center of Excellence in Translational Science, Janssen
Yan Wang
Merck Sharp & Dohme
Piu Wong
HiFiBio Therapeutics
Hermi Sumatoh
ImmunoScape
Michael Fehlings
ImmunoScape Pte Ltd, Singapore https://orcid.org/0000-0002-0384-8408
Alessandra Nardin

ImmunoScape
Liang Liu
Macau University of Science and Technology
Yabing Cao
Kiang Wu Hospital
Elaine Leung (lhleung@must.edu.mo)
Macau Institute for Applied Research in Medicine and Health, State Key Laboratory of Quality Research in Chinese Medicine

---

Article

Keywords: Non-small cell lung cancer, Anti-PD-1, CyTOF, Longitudinal analysis

Posted Date: September 16th, 2021

DOI: https://doi.org/10.21203/rs.3.rs-863654/v1

Version of Record: A version of this preprint was published at Nature Communications on August 22nd, 2023. See the published version at https://doi.org/10.1038/s41467-023-40631-0.

Abstract

The response to immunotherapy could be better predicted by using a wide set of biomarkers, including serum tumor markers; however, robust immune markers associated with efficacy have yet to be validated. In this study, changes in immune cell subsets from NSCLC patients treated with anti-PD1 therapy were longitudinally monitored by high-dimensional cytometry by time of flight (CyTOF) and Meso Scale Discovery (MSD) multi-cytokines kits. The frequencies of circulating $CD8^+$ and $CD8^+CD101^{hi}TIM3^+$ (CCT T) subsets were significantly correlated with clinical response and survival. Enrichment of these populations in peripheral blood mononuclear cells (PBMCs) indicated a poor clinical response to ICB therapy. Cell function assays revealed that these subsets were remarkably impaired, which supported the poor outcomes observed. Additionally, longitudinal analysis showed that KLRG1 expression and cytokines were associated with the response to therapy. Overall, our results provide novel potential biomarkers for guiding the management of NSCLC patients eligible to anti-PD-1 therapy, and contribute insights for new therapeutic strategies.

Introduction

Immune checkpoint blockade (ICB) therapy is known to produce durable clinical responses in a select group of non-small cell lung cancer (NSCLC) patients; therefore, early identification of progression is critical for patient selection. To achieve better effectiveness with ICB therapy, predictive biomarkers are critically needed. Several predictors of the response to PD-1 blockade have been reported, such as the presence of tumor-infiltrating T cells, high PD-L1 expression in biopsies, microsatellite instability (MSI) and the tumor mutational burden (TMB) [1, 2, 3]. However, these biomarkers are hampered by the limited longitudinal observation window, the small number of parameters and the lack of systematic, unbiased bioinformatic pipelines, which has resulted in a paucity of predictive biomarkers to date. Longitudinal investigation is important to trace markers associated with acquired resistance since the anti-PD1-mediated immune response is dynamic during treatment cycles. However, it is unclear whether noninvasive approaches, such as PBMC profiling, can be used to predict responses to ICB therapy by identifying the relevant responding cell types, which could provide insights for understanding the underlying immunological mechanisms of primary and acquired resistance.

Here, we combined high-dimensional CyTOF and multiplex cytokine approaches for the first time to longitudinally analyze twenty-five patients diagnosed with NSCLC over at least 30 months. To better understand the predictive and resistant biomarkers associated with anti-PD-1 treatment, immunophenotyping, molecular analysis and functional characterization of immune populations were performed. The findings in this study could provide insights to guide precision therapy and elucidate the underlying mechanism of treatment resistance.

Results

Enrichment of $CD8^+$ and CCT T subsets predicts the efficacy of anti-PD-1 therapy. To monitor immune cell responses induced by PD-1-targeted therapy, PBMCs were isolated and analyzed by CyTOF. Sixteen healthy donors (HDs) and twenty-five patients with NSCLC were enrolled (Figure S1, Table S1). Patient clinical response was determined on the basis of immune response evaluation criteria in solid tumors (RECIST) criteria (Figure S2), consistent with published trials in lung cancer [4, 5].

To identify the predictive cell subsets, immune cells were subsequently clustered based on 40 leukocyte antigens (Table S2), and the differences between responding and non-responding patients were examined (Figures S3-S7). Responders had much lower frequencies of $CD8^+$ T cell subtypes, especially $CD8^+CD101^{hi}TIM3^+$ (CCT T) cells, which have been associated with exhausted cells [6, 7] (Figure 1a and 1b).

Longitudinal analysis (Figures S8 and S9) showed that both $CD8^+$ T cells and CCT T cells remained at low levels in most responders during the 10 treatment cycles (Figure 1c). We next assessed whether differences in $CD8^+$ and CCT subtype T cells at baseline may be associated with patient clinical outcomes. As shown in Figure 1d, 38% of the patients with a high frequency (cutoff is median value) of $CD8^+$ T cells had progressive disease (PD), higher than the 28% of the patients with a low frequency of these major immune cells. This phenomenon was more significant for the CCT subtype; 63% of the patients with a high frequency and 23% of those with a low frequency were defined as having PD. Therefore, whether the CCT subtype of $CD8^+$ T cells can serve as a biomarker predictive of progression-free survival (PFS) in this cohort of NSCLC patients was further studied. As shown in Figure 1e, patients with a high level of $CD8^+$ T cells exhibited worse PFS (7 months) than those with a low level of $CD8^+$ T cells (13 months). This result indicated that higher frequencies of $CD8^+$ subtypes and CCT T subtype were associated with unfavorable outcomes.

$CD8^+$ and CCT T cell exhibited specific phenotype in NSCLC patients before and after anti-PD-1 therapy. To explore the treatment-associated changes in phenotype and compare patients with HDs, leukocyte antigens related to $CD8^+$ and CCT T cells were comprehensively investigated (Figures S10-S12). As shown in Figure 2a, Granzyme B and T-bet, which are functional markers in cytotoxic T cells, were remarkably upregulated in responder $CD8^+$ T cells. A similar trend of Granzyme B and T-bet was observed in CCT T cells (Figure 2b), in which the CD27 level was significantly decreased. Furthermore, killer cell lectin-like receptor subfamily G, member 1 (KLRG1), which is enhanced in cytotoxic and terminal effector $CD8^+$ T cells [8], was remarkably increased in CCT cells from responders at baseline (Figure 2c).

Longitudinally (Figures S13 and S14), the levels of Granzyme B and T-bet were consistently higher in $CD8^+$ and CCT T cells of responders (Figure 3a and 3b). In addition, KLRG1 levels in CCT T cells was higher in responders and could effectively discriminate responders from non-responders even at baseline (Figure 3b). Furthermore, we correlated predictive T cell subtypes with patient tumor clinical characteristics, such as CT scan results for the tumor burden [9]. We applied a practical approach

to estimate the tumor burden by using the major measurable tumor lesion on pretreatment PET-CT scan images of NSCLC patients. Indeed, a higher tumor burden was associated with higher frequencies of $CD27^+CD8^+$ T cells and $CD27^+$CCT T cells, regardless of whether treatment was given (Figure 3c). Altogether, these findings indicated that the different phenotypes of $CD8^+$ and CCT T cells between responders and non-responders may be predictive of the clinical efficacy of anti-PD-1 therapy.

The functional properties of T cells were impaired in non-responders. Next, we correlated cytokine levels with immune subpopulations to determine their functional properties (Figure 4, Figures S15-S17). Significantly decreased levels of plasma Eotaxin-3, IL-1β, IL-23, TNF-α, MDC and MCP-4 were observed in responders versus non-responders (Figure 4a, S18). Furthermore, we stimulated patient PBMCs with a T cell stimulator (anti-CD3/CD28 or PMA) *in vitro* and collected the supernatant to measure the levels of secreted cytokines. In general, cytokines including IL-1β, IL-2, IL-8, IL-22 and MCP-1 were higher after stimulation in responders compared with non-responders (Figure 4b and Figure S19). We further tested $CD8^+$ and CCT T cell cluster-related cytokines in PFS analysis. High levels of IL-22 at baseline was remarkably associated with prolonged PFS (Figure 4c). The results suggest that the anticancer activity of T cells in non-responders may have been compromised and associated with patient PFS.

Discussion

To establish reliable criteria for predicting the clinical response to anti-PD-1 therapy, a combination of high-dimensional CyTOF and MSD multiplex cytokine longitudinal analysis was applied to PBMCs collected from a cohort of 25 Chinese NSCLC patients who received ICB therapy. To date, this is the longest follow-up time (30 months) in an NSCLC report with high-dimensional investigations. We proposed a noninvasive, feasible approach for tracking the changes in immune subsets, which can help to accurately distinguish responders and non-responders. The repertoire of surface molecules that are preferentially expressed on dysfunctional T cells has been extensively studied, such as TIM3, PD-1, CTLA4, LAG3LAG3 and TIGIT [10]. We discovered that the increase of $CD8^+$ T cell frequency is associated with a worse clinical response to anti-PD-1 therapy, which contradicts the conventional understanding that $CD8^+$ T cells are expected to be associated with a favorable prognosis. However, it has been reported that $CD8^+$ T cells transition through the blood and migrate into the tumor site [11]. $CD8^+$ T cell expansion and migration result in a higher number of infiltrating tumor-specific $CD8^+$ T cells, which contribute to clinical responses to PD-1 therapy [12,13]. T cell infiltration can be a positive prognostic indicator in a variety of cancers [14]. Moreover, we identified for the first time that the CCT T cell ($CD8^+CD101^{hi}TIM3^+$ T cells) subtype was predictive of worse ICB therapeutic efficacy. It has been reported that the irreversible TIM3 and CD101 expression is an hallmark of $CD8^+$ T cells exhaustion during infection [15,16], which is consistent with our results. We observed that the number of dysfunctional CCT T cells was significantly higher in non-responders. Thus, we propose that exhausted T cells would harbor a lower ability to migrate and function.

Another key insight from our research was derived from investigating the connection between cell subsets and cytokine secretion potential. Granzyme B is a serine protease released by $CD8^+$ T cells and natural killer cells and functions as a downstream effector of tumor cytotoxic T cells [17, 18]. A recent study found that alterations in the Granzyme B gene (GZMB/H) negatively predicted ICB efficacy in nasopharyngeal cancer patients [19]. Thus, the role of Granzyme B protein as a biomarker was investigated in our study. T-bet is an immune cell-specific member of the T-box family of transcription factors and plays a pivotal role in infectious, inflammatory and autoimmune conditions as the master regulator of effector T-cell activation [20]. It has been reported that patients' overall survival was significantly improved by immunotherapy in patients with high T-bet-expressing T cells [21,22]. We demonstrated here that the levels of Granzyme B and T-bet were higher in $CD8^+$ and CCT T cells of responders (Figure 3a and 3b), which suggests indicated the deficiency of these two factors may be linked to CD8 T cell exhaustion and failure to respond to anti-PD-1 therapy. Most interestingly, the induction of KLRG1 in CCT T cells after one cycle of anti-PD1 treatment was shown to be positively correlated with the efficacy of anti-PD-1 therapy for the first time. The function of KLRG1 is well known to be directly involved in T cell activation [8, 23]. Consequently, $KLRG1^+$ CCT T cells could represent an activated super killing population with more cytotoxic effector function and a senescent phenotype. To fully understand the immune status in the tumor microenvironment, we further tested the association of cytokines with anti-PD-1 therapy. IL-1β, IL-2, IL-22, IL-23 and TNF-α have been demonstrated to be associated with better prognosis of NSCLC patients.

In conclusion, we have identified a novel set of specific immune subtypes that are enriched in non-responders to ICB therapy. We further elucidated the connection of immune cells with their correlated cytokines. Unlike using biopsy, we provide a noninvasive and feasible method for early and timely monitoring of treatment response. For future clinical utilization, we suggest combining our findings with widely used clinical parameters to provide more accurate information to predict ICB treatment efficacy.

Materials And Methods

Unique Chinese lung cancer patients

Patient blood samples and information were collected at Macau Kiang Wu Hospital, and all patients signed an informed consent form. For lung cancer patients, the treatment course of pembrolizumab was dependent on efficacy, but the average cycle was approximately 3-4 weeks, and the patients received 6 treatment courses. Clinical pathological data, routine CT scans, and immunohistochemistry (IHC) data were recorded. Immunological profiles and patient response correlation analysis were applied. The percentage of the immune cell subpopulations between the patients and HDs was analyzed. In addition, the correlations of cell subsets with PD-L1 expression (determined by IHC and routine pathology practice) and treatment response were analyzed. Ethic code number: (2018-007).

Clinical sample collection and PBMC isolation

Whole blood from patients and HDs was collected. Blood samples were stored in EDTA-coated tubes. Human PBMCs were isolated using a density gradient technique (Ficoll-Paque PLUS from GE Healthcare Life Sciences). Seven milliliters of blood was mixed with 7 ml of a balanced salt solution, normally PBS. The mixed blood solution was overlayed on top of 15 ml of Ficoll-Paque PLUS. The mixture was centrifuged at 300 g for 15 min at room temperature (RT). During this step, the granulocytes, platelets, and red blood cells (RBCs) pelleted at the bottom of the tube, and the PBMCs floated over the Ficoll-Paque PLUS layer. PBMCs were collected from the Ficoll-plasma interface. PBMCs were washed twice with PBS at 300 g for 5 min. The total number of PBMCs collected from each sample was counted and recorded. Isolated PBMCs were cryopreserved and stored at -80 °C according to a standard protocol.

Cytokine assays

The wells of MSD 384-well plates (Meso Scale Discovery) were coated overnight at 4 °C with 10 µL of coating antibody in carbonate-bicarbonate coating buffer (15 mM Na_2CO_3/35 mM $NaHCO_3$, pH 9.6). The plates were then washed three times with 35 µL of wash buffer (0.2% Tween-20 in PBS) per well and blocked with 35 µL of blocking buffer (2% Probumin/0.2% Tween-20 in PBS) per well for 1 h at RT with rotational shaking. Plasma and cell culture supernatant samples were diluted to the desired concentrations in a mixture of aggregation buffer and at least 50% blocking buffer. After an additional washing step, 10 µL of sample was transferred to each well of the antibody-coated MSD plate and incubated with shaking for 1 h at RT. After aspiration of the samples and four washes with 35 µL of wash buffer each time, 10 µL of primary detection antibody (shown in the table below) was added to each well and incubated with shaking for 1 h at RT. For non-labeled primary detection antibodies, 10 µL of goat anti-mouse SULFO-TAG-labeled secondary detection antibodies (1:1,000 in blocking buffer; Meso Scale Discovery) was added to each well after an additional washing step and incubated with shaking for 1 h at RT. After washing three times with wash buffer, 35 µL of read buffer T with surfactant was added to each well, and the plate was imaged on a Sector Imager 6000 (Meso Scale Discovery) according to the manufacturers' instructions for the V-PLEX Human Cytokine-44 Plex Kit, U-PLEX Human TGF-β1-Kit and R-PLEX Human Granzyme B-Kit.

T cell stimulation

Physiological activation of human T cells was achieved with Dynabeads Human T-Activator CD3/CD28. First, Dynabeads Human T-Activator CD3/CD28 were resuspended in the vial. Then, the desired volume of Dynabeads was transferred to a tube. An equal volume of buffer were added and mixed. Next, the tube was placed on a magnet for 1 min, and the supernatant was discarded. The Dynabeads were resuspended in a volume of culture medium equal to the initial volume of Dynabeads taken from the vial. Then, T cell stimulation was performed with 5×10^5 PBMCs in 100-200 µl of medium in a 96-well tissue culture plate. Two microliters of Dynabeads Human T-Activator CD3/CD28 was added to obtain a bead-to-cell ratio of 1:1. Finally, the plate was incubated in a humidified CO2 incubator at 37 °C for 72 h, and the cell culture supernatant was harvested for further MSD tests.

Another simulator, PMA, was also used for shorter incubations to increase the levels of cytokine production. T cell stimulation was performed with 5×10^5 PBMCs in 100-200 µl of medium in a 96-well tissue culture plate. Then, 12.5 ng/ml PMA was added to each well. The plate was incubated in a humidified CO_2 incubator at 37 °C for 18 h, and the cell culture supernatant was harvested for further MSD tests.

CyTOF examination of immune subpopulations

After PBMC collection, samples were cryopreserved. Approximately 5-6 million cells were shipped to a CyTOF service provider (Immunoscape, Singapore). Forty major and minor immune markers were analyzed simultaneously (the target panel composition is detailed in Table S2). Antibodies were labeled with an optimal combination of metals. HD samples were run in parallel with patient samples. Samples were thawed at 37 °C, transferred into complete RPMI medium supplemented with 10% fetal calf serum (hiFCS), 1% penicillin/streptomycin/glutamine, 10 mM HEPES, and 55 µM 2-mercaptoethanol (2-ME) supplemented with 50 U/ml benzonase (Sigma) and immediately processed for staining. Since considerable variation in sample quality was observed, a sorting step was implemented for some of the samples to overcome poor sample quality, which might have resulted in higher background signals or cell loss during sample staining. Therefore, cells were stained with fluorophore-conjugated (allophycocyanin, APC) anti-human CD45 antibodies (BioLegend) and a Live/Dead (ThermoFisher) cell stain on ice for 20 min. Subsequently, the cells were washed twice, and live CD45-positive lymphocytes were sorted using a FACSAria II flow cytometry-based cell sorter (Beckton Dickinson). Sorted cells were then added to HD PBMCs to reach a minimum of 3×10^6 cells per staining condition.

For antibody staining, samples were stained with a primary fluorophore-labeled anti-TCRγδ antibody for 30 min on ice, washed twice, and then incubated with 50 µl of a metal-labeled antibody cocktail for 30 min on ice, followed by fixation in 2% paraformaldehyde in PBS overnight at 4 °C. The samples were then washed once in permeabilization buffer and barcoded with a unique combination of two distinct barcodes for 30 min on ice. The cells were washed once, incubated in cytometry buffer for 5 min, and then suspended in 250 nM iridium intercalator (DNA staining) in 2% paraformaldehyde/PBS at RT. The cells were washed, and the samples from each patient were pooled together with 1% polystyrene bead standards (EQ™ Four element calibration beads, Fluidigm) for acquisition on a HELIOS mass cytometer (Fluidigm).

The signals for each parameter were normalized based on the equilibration beads (EQ™ Four Element Calibration Beads, Fluidigm) added to each sample. Since mass cytometry provides absolute quantitation of isotopic metal labels bound to each cell, metal-conjugated antibodies that are not detected on single cells are measured as zero values. To improve the visualization of cells displayed in a compressed 2-dimensional dot plot, we randomized the signal of zero into values between 0 and 1 using R with the flow Core package; this data processing does not affect further downstream analysis. Each sample was manually debarcoded and then gated on live $CD8^+$ T cells ($CD45^+DNA^+cisplatin^-CD3^+$ cells) after gating out natural killer (NK) cells ($CD56^+CD16^+$), monocytes ($CD14^+$) and TCRγδ cells

($CD3^+TCR\gamma\delta^+$) using FlowJo software (TreeStar Inc.). Correlation or trend analysis was performed to correlate immune profiles with responders and non-responders. Bioinformatic analysis was performed using phenotypic profiling involving UMAP dimensionality reduction and clustering algorithms. Statistical modeling was performed to broadly assess immunotherapy effects.

SPSS and statistical analysis

All experiments were performed at least in triplicate. A t-test was used to compare a single experimental group with a control group. One-way ANOVA was used for multiple-group comparisons. SPSS software was used for clinicopathological parameter analysis, and tools such as the chi-square test were used. The two-sided significance level was set at $p<0.05$.

Declarations

AUTHOR CONTRIBUTION

Contributors LL, YBC and ELHL contributed to research design. RZL and YBC contributed to data collection. RZL, XXF, ZBJ, JMH, LYW, YF, HMX, LZ, PG, YW, PW, HS, MF and AN analyzed and interpreted data. RZL and XXF wrote the report, which was critically reviewed and revised by LL, YBC and ELHL. All authors reviewed and approved the final report.

ACKNOWLEDGEMENTS

We thank the patients and their families. The research leading to these results has received funding from the Macau Science and Technology Development Fund (Project no: 0096/2018/A3 & 001/2020/ALC), NSFC overseas and Hong Kong and Macao scholars cooperative research fund project (Project no: 81828013) and Janssen therapeutic fund (Project code: ICD#1101175) as well as The 2020 Guangdong Provincial Science and Technology Innovation Strategy Special Fund (Guangdong-Hong Kong-Macau Joint Lab) (Project no: 2020B1212030006).

ETHIC APPROVAL

This study was approved by Kiang Wu Hospital under the approval number 2018-007.

CONFLICTS OF INTEREST

All authors declare that they have no conflicts of interest.

References

1. Gettinger RHJSMKGFOHMGJSDMJPS. Predictive correlates of response to the anti-PD-L1 antibody MPDL3280A in cancer patients. *Nature* 2014, **515**(7528)**:** 563.

2. Alisha N West; Manuel Carmona; Christine Kivork; Elizabeth Seja; Grace Cherry; Antonio J Gutierrez; Tristan R Grogan; Christine Mateus; Gorana Tomasic; John A Glaspy; Ryan O Emerson; Harlan Robins; Robert H Pierce; David A Elashoff; Caroline Robert; Antoni Ribas PCTCLHJHYIPSEJMTLRBCMSGHVC. PD-1 blockade induces responses by inhibiting adaptive immune resistance. *Nature* 2014, **515**(7528)**:** 568.

3. Verma V, Shrimali RK, Ahmad S, Dai W, Wang H, Lu S*, et al.* PD-1 blockade in subprimed CD8 cells induces dysfunctional PD-1(+)CD38(hi) cells and anti-PD-1 resistance. *Nat Immunol* 2019, **20**(9)**:** 1231-1243.

4. Robert C, Schachter J, Long GV, Arance A, Ribas A. Pembrolizumab versus Ipilimumab in Advanced Melanoma. *New England Journal of Medicine* 2015, **372**(26)**:** 2521-2532.

5. Ribas A, Puzanov I, Dummer R, Schadendorf D, Hamid O, Robert C*, et al.* Pembrolizumab versus investigator-choice chemotherapy for ipilimumab-refractory melanoma (KEYNOTE-002): a randomised, controlled, phase 2 trial. *The Lancet Oncology* 2015, **16**(8)**:** 908-918.

6. Zander R, Schauder D, Xin G, Nguyen C, Cui W. CD4+ T Cell Help Is Required for the Formation of a Cytolytic CD8+ T Cell Subset that Protects against Chronic Infection and Cancer. *Immunity* 2019, **51**(6).

7. Hudson WH, Gensheimer J, Hashimoto M, Wieland A, Valanparambil RM, Li P*, et al.* Proliferating Transitory T Cells with an Effector-like Transcriptional Signature Emerge from PD-1+ Stem-like CD8+ T Cells during Chronic Infection - ScienceDirect. *Immunity* 2019.

8. Herndler-Brandstetter D, Ishigame H, Shinnakasu R, Plajer V, Stecher C, Zhao J*, et al.* KLRG1(+) Effector CD8(+) T Cells Lose KLRG1, Differentiate into All Memory T Cell Lineages, and Convey Enhanced Protective Immunity. *Immunity* 2018, **48**(4)**:** 716-729 e718.

9. Huang AC PM, Orlowski RJ, Mick R, Bengsch B, Manne S, Xu W, Harmon S, Giles JR, Wenz B, Adamow M, Kuk D, Panageas KS, Carrera C, Wong P, Quagliarello F, Wubbenhorst B, D'Andrea K, Pauken KE, Herati RS, Staupe RP, Schenkel JM, McGettigan S, Kothari S, George SM, Vonderheide RH, Amaravadi

RK, Karakousis GC, Schuchter LM, Xu X, Nathanson KL, Wolchok JD, Gangadhar TC, Wherry EJ. . T-cell invigoration to tumour burden ratio associated with anti-PD-1 response. . *Nature* 2017 May 4, **545**(7652)**:** 60-65. .

10. Kamphorst AO, Pillai RN, Yang S, Nasti TH, Ramalingam SS. Proliferation of PD-1+ CD8 T cells in peripheral blood after PD-1–targeted therapy in lung cancer patients. *Proc Natl Acad Sci U S A* 2017, **114**(19)**:** 4993-4998.

11. Tumeh PC, Harview CL, Yearley JH, Shintaku IP, Taylor EJM, Robert L*, et al.* PD-1 blockade induces responses by inhibiting adaptive immune resistance. *Nature* 2014, **515**(7528)**:** 568-571.

12. Chen PL, Roh W, Reuben A, Cooper ZA, Wargo JA. Analysis of Immune Signatures in Longitudinal Tumor Samples Yields Insight into Biomarkers of Response and Mechanisms of Resistance to Immune Checkpoint Blockade. *Cancer Discovery* 2016, **6**(8).

13. Ribas A, Shin DS, Zaretsky J, Frederiksen J, Cornish A, Avramis E*, et al.* PD-1 Blockade Expands Intratumoral Memory T Cells. *Cancer Immunology Research* 2016**:** 194.

14. Kluger HM, Zito CR, Barr M, Baine MK, Jilaveanu LB. Characterization of PD-L1 Expression and Associated T-cell Infiltrates in Metastatic Melanoma Samples from Variable Anatomic Sites. *Clinical Cancer Research* 2015, **21**(13)**:** 3052.

15. Philip M, Fairchild L, Sun L, Horste EL, Amara SC, Shakiba M*, et al.* Chromatin states define tumour-specific T cell dysfunction and reprogramming. *Nature* 2017, **545**(7655)**:** 452.

16. Hudson WH, Gensheimer J, Hashimoto M, Wieland A, Valanparambil RM, Li P*, et al.* Proliferating Transitory T Cells with an Effector-like Transcriptional Signature Emerge from PD-1(+) Stem-like CD8(+) T Cells during Chronic Infection. *Immunity* 2019, **51**(6)**:** 1043-1058 e1044.

17. Nguyen A, Ramesh A, Kumar S, Nandi D, Brouillard A, Wells A*, et al.* Granzyme B nanoreporter for early monitoring of tumor response to immunotherapy. *Sci Adv* 2020, **6**(40).

18. Hurkmans DP, Basak EA, Schepers N, Oomen-De Hoop E, Van der Leest CH, El Bouazzaoui S*, et al.* Granzyme B is correlated with clinical outcome after PD-1 blockade in patients with stage IV non-small-cell lung cancer. *J Immunother Cancer* 2020, **8**(1).

19. Ma Y, Chen X, Wang A, Zhao H, Lin Q, Bao H*, et al.* Copy number loss in granzyme genes confers resistance to immune checkpoint inhibitor in nasopharyngeal carcinoma. *J Immunother Cancer* 2021, **9**(3).

20. Pritchard GH, Kedl RM, Hunter CA. The evolving role of T-bet in resistance to infection. *Nat Rev Immunol* 2019, **19**(6)**:** 398-410.

21. Kallies A, Good-Jacobson KL. Transcription Factor T-bet Orchestrates Lineage Development and Function in the Immune System. *Trends Immunol* 2017, **38**(4)**:** 287-297.

22. Egelston CA, Avalos C, Tu TY, Simons DL, Jimenez G, Jung JY*, et al.* Human breast tumor-infiltrating CD8(+) T cells retain polyfunctionality despite PD-1 expression. *Nat Commun* 2018, **9**(1)**:** 4297.

23. Burrack AL, Spartz EJ, Raynor JF, Wang I, Olson M, Stromnes IM. Combination PD-1 and PD-L1 Blockade Promotes Durable Neoantigen-Specific T Cell-Mediated Immunity in Pancreatic Ductal Adenocarcinoma. *Cell Rep* 2019, **28**(8)**:** 2140-2155 e2146.

Figures

Figure 1

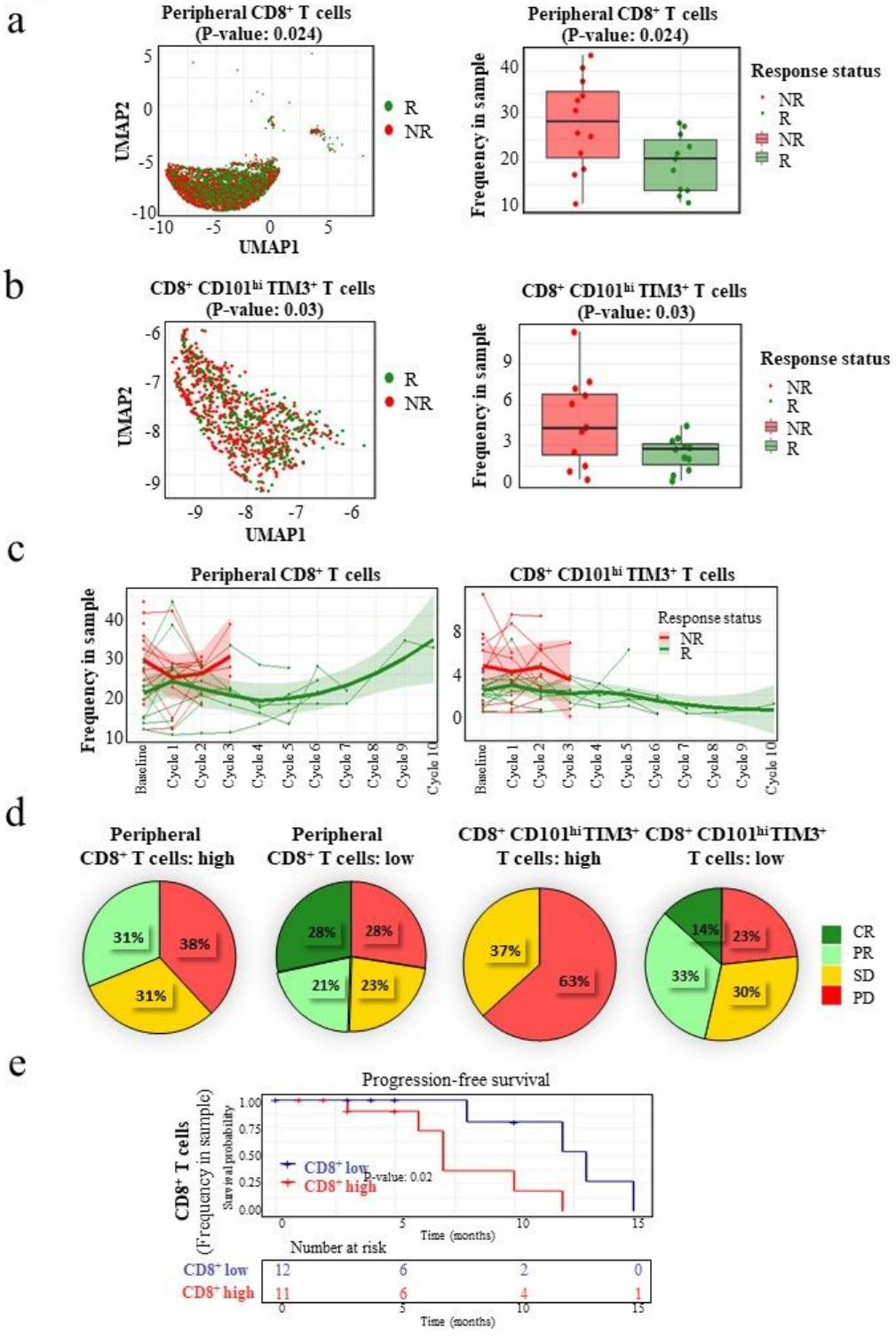

Figure 1

The enrichment of CD8+ and CCT subsets predict the efficacy of anti-PD-1 therapy. a. The frequency of CD8+ T cells from responders' PBMC were lower than that of non-responders. b. Much lower frequencies of CCT subtype were observed in responders' PBMC as well. c. By longitudinal analysis, both CD8+ T cells and CCT T cells remained at low levels in most responders during the 10 treatment cycles. d. High frequency of CD8+ T cells and CCT T cells was correlated with bad prognosis after the treatment of anti-

PD1 therapy. e. High level of total CD8+ T cell exhibited worse median PFS. Box plots represent the IQR, with the horizontal line indicating the median. p-value in PFS analysis was examined by the log-rank test. Other p-values were calculated using two-sided t-tests and were corrected for the multiple comparison using the Benjamini-Hochberg adjustment. R: responder. NR: non-responder. CR: complete response. PR: partial response. SD: stable disease. PD: progressive disease.

Figure 2

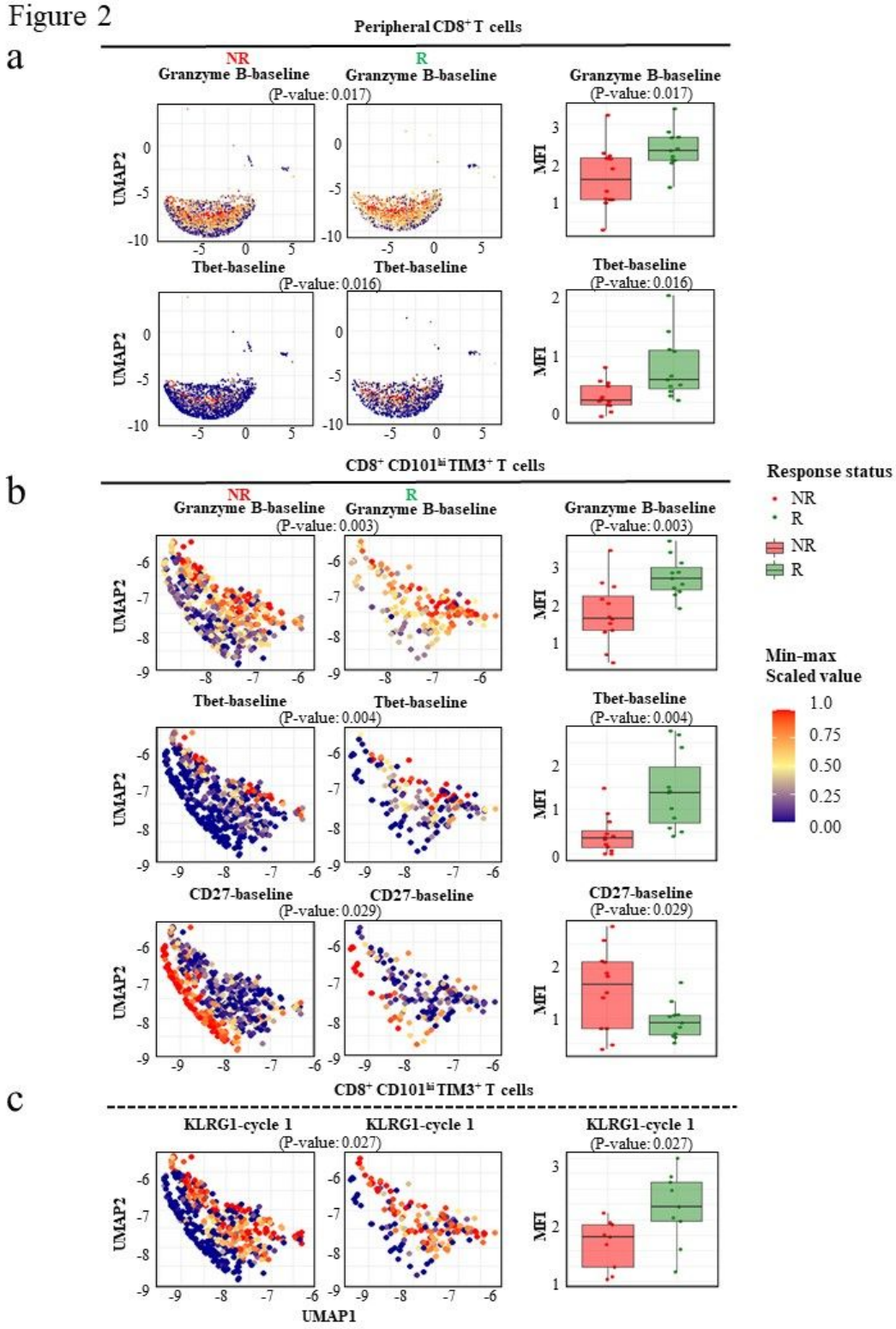

Figure 2

CD8+ and CCT T cells exhibit specific antigens in NSCLC patients before and after anti-PD-1 therapy. a. Granzyme B and Tbet were remarkably upregulated in responders' CD8+ T cells. b. Similar trend of Granzyme B and Tbet were observed in CCT T cells, in which the CD27 level was significantly decreased. c. KLRG1 was remarkably increased as well in responders' CCT cells. All p-values were calculated using two-sided t-tests.

Figure 3

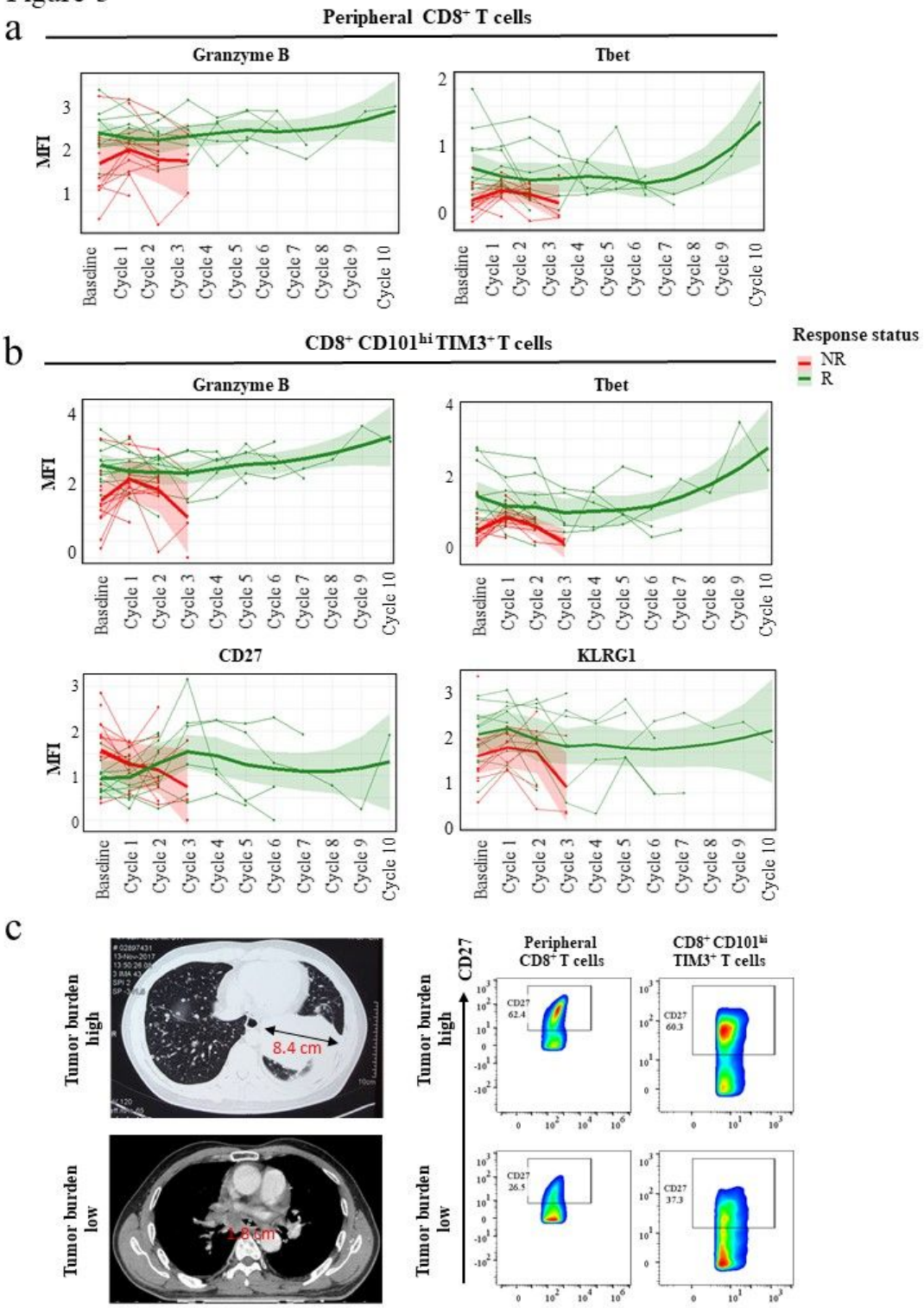

Figure 3

Different phenotypes of CD8+ and CCT T cells between responders and non-responders were predictive of the clinical efficacy of anti-PD-1 therapy. a and b. Longitudinally the levels of Granzyme B and Tbet were consistently higher in responder CD8+ and CCT T cells. c. A higher tumor burden was associated with higher frequencies of CD8+CD27+ T cells and CCT T cells.

Figure 4

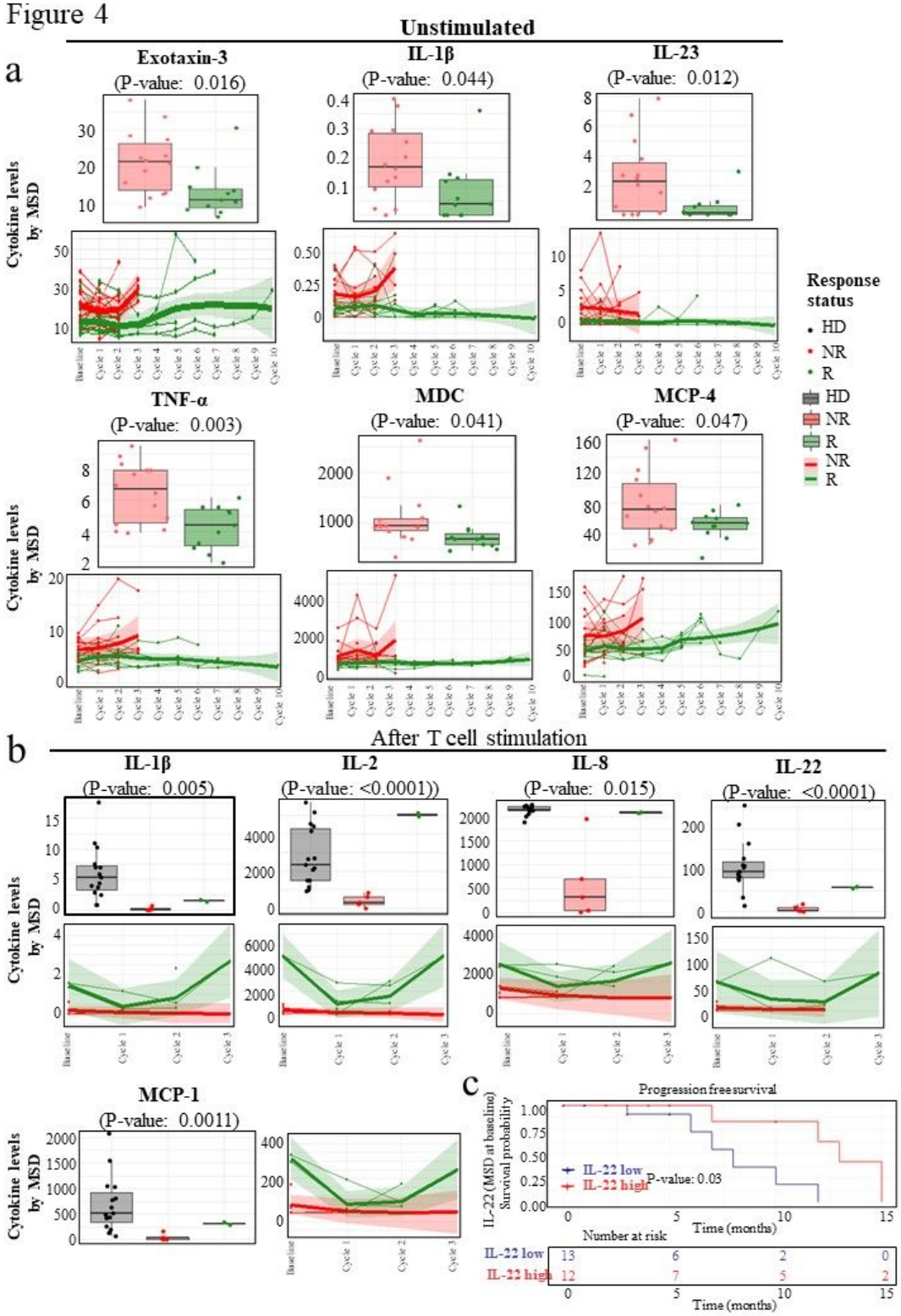

Figure 4

The functional properties of T cells were impaired in non-responders. a. Decreased levels of plasma Eotaxin-3, IL-1β, IL-23, TNF-α, MDC and MCP-4 were observed in responders versus non-responders. b. In stimulated patient PBMCs, secreted cytokines, including IL-1β, IL-2, IL-8, IL-22 and MCP-1, were significantly increased in responders compared with non-responders. c. High levels of IL-22 remarkably contributed to prolonged PFS. p-value in PFS analysis was examined by the log-rank test. Other p-values were calculated using two-sided t-tests.

Supplementary Files

This is a list of supplementary files associated with this preprint. Click to download.

- Supplementarydata.pdf